

Supporting Information for

A porous coordination framework for highly sensitive and selective solid-phase microextraction of non-polar volatile organic compounds

Chun-Ting He, Jing-Yu Tian, Si-Yang Liu, Gangfeng Ouyang, Jie-Peng Zhang*, Xiao-Ming Chen

MOE Key Laboratory of Bioinorganic and Synthetic Chemistry, State Key Laboratory of Optoelectronic Materials and Technologies, School of Chemistry & Chemical Engineering, Sun Yat-Sen University, Guangzhou 510275, P. R. China.

*E-mail: zhangjp7@mail.sysu.edu.cn

Supplementary Index

1. Glossary of abbreviations used in this paper.
2. Experimental section
3. Computational details
4. Table S1. Crystallographic data and structure refinement details for MAF-X8.
5. Fig. S1. Perspective view of coordination environments of MAF-X8.
6. Fig. S2. Perspective view of the structure of mesitylene loaded MAF-X8.
7. Fig. S3. PXRD patterns for MAF-X8.
8. Fig. S4. TGA curve for MAF-X8.
9. Fig. S5. N₂ sorption isotherm of MAF-X8 at 77 K.
10. Fig. S6. PXRD patterns for activated MAF-X8 exposed to saturated water vapor for different time and subsequent restoration of the water-treated samples by MeOH vapor or by direct heating.
11. Fig. S7. Adsorption and desorption kinetics of the MAF-X8 coated SPME fiber.
12. Table S2. The limits of detection (LODs), linear range and the relative standard deviation (RSD).
13. Table S3. Comparison of the major parameters for various SPME fibers in determination of BTEX compounds.
14. Fig. S8. Comparison of major parameters for different fibers in determination of BTEX compounds.
15. Fig. S9. Comparison of the extraction efficiencies of MAF-X8 coated fiber and commercial SPME fibers. The error bar shows the standard deviation of the mean.
16. Table S4. Plotted data for Fig. 4 and Fig. 5.
17. Table S5. The theoretical/observed saturation/maximum uptakes of mesitylene, toluene and 2-chlorophenol.
18. Fig. S10. TGA curves for MAF-X8 after exposed to 2-chlorophenol or toluene vapor for different time.
19. References

Glossary of abbreviations used in this paper.

Abbreviations	Name
PCPs	porous coordination polymers
MOFs	metal-organic frameworks
SPME	solid-phase microextraction
MAFs	metal azolate frameworks
TGA	Thermogravimetric analysis
PXRD	powder X-ray diffraction
DMA	dimethylacetamide
GC	gas chromatography
H ₂ mpba	4-(3,5-dimethylpyrazol-4-yl)benzoic acid
LODs	limits of detection
RSD	relative standard deviation
PDMS	polydimethylsiloxane
DVB	divinylbenzene
MM	molecular mechanics
DFT	density-functional theory

Experimental section

General information

The ligand 4-(3,5-dimethylpyrazol-4-yl)benzoic acid (H_2mpba) was synthesized according to the literature.^{S1} The nonpolar standard BTEX compounds including benzene, toluene, ethylbenzene, *o*-xylene, and polar standard Phenols including 2-chlorophenol, *p*-cresol, 2-nitrophenol, 2,4-dichlorophenol, and 2,4,6-trichlorophenol were purchased from Alfa Aesar and dissolved in methanol (high performance liquid chromatography grade) to make stock solutions at a concentration of 1 mg/mL for each compound. All commercially available reagents and solvents were used as received without further purification. The SPME manual holder and commercial fibers (100 μ m PDMS and 65 μ m PDMS/DVB) were obtained from Supelco.

Elemental analyses (C, H, N) were obtained by a Vario EL elemental analyzer. All the Powder X-ray diffraction (PXRD) data was recorded on a Bruker D8 ADVANCE X-ray powder diffractometer (Cu $K\alpha$). Thermogravimetric analysis (TGA) was performed using a TGA Q50 instrument. Each sample was heated from room temperature to 700 °C at a rate of 5.0 °C/min under N_2 atmosphere. Measurements of N_2 sorption isotherms were performed on a Micromeritics ASAP 2020M instrument. Before gas sorption experiments, the as-synthesized samples were placed in a quartz tube and dried under high vacuum at 180 °C for 10 h to remove the remnant solvent molecules.

Syntheses of MAF-X8

Single crystals: A mixture of H_2mpba (0.022 g, 0.1 mmol), $Zn(NO_3)_2 \cdot 6H_2O$ (0.030 g, 0.1 mmol), DMA (0.1 mL), EtOH (2.5 mL), H_2O (2.5 mL), and mesitylene (1.0 mL) was sealed in a 10-mL Teflon-lined stainless steel container and kept at 120 °C for 3 days, followed by being cooled to room temperature at a rate of 5 °C·h⁻¹. Colorless prismatic crystals [$Zn(mpba)$] $\cdot 0.76C_9H_{12}$ were obtained (ca. 0.027 g, 54% yield based on Zn). EA calcd (%) for

[Zn(mpba)]·0.76C₉H₁₂ (C_{18.87}H_{19.16}N₂O₂Zn): C 61.03, H 5.20, N 7.54. Found: C 61.23, H 5.302, N 7.26.

Bulk microcrystalline powder: A mixture of H₂mpba (0.5 mmol, 0.108 g), Zn(NO₃)₂·6H₂O (0.5 mmol, 0.150 g), DMA (3.0 mL), and MeOH (9.0 mL) was sealed in a 15-mL Teflon-lined stainless steel container and kept at 120 °C for 3 days. After cooling to room temperature, washed by DMA and MeOH for several times, white powders were obtained (0.157 g, 62% yield based on Zn). Guest-free samples were obtained by heating the bulk sample at 200 °C for 30 min at N₂ atmosphere. EA calcd (%) for [Zn(mpba)] (C₁₂H₁₀N₂O₂Zn): C 51.55, H 3.60, N 10.02. Found: C 51.26, H 3.58, N 9.97.

SPME fibers: Firstly, the stainless steel wires ($d = 0.120$ mm, $l = 5$ cm) were washed by acetone to remove the exterior organic impurity. Then, one end of the stainless steel wire (about 3 cm length) was immersed in aqua regia for 15 min in order to generate a fresh, rough surface. Afterwards, the etched stainless steel wire was washed by ultrapure water until pH = 7 and dried in desiccator at room temperature. A 1:1 mixture of H₂mpba (0.1 mmol) and Zn(NO₃)₂·6H₂O (0.1 mmol) in DMA (1.5 mL) and MeOH (4.5 mL) was sealed in a 10-mL Teflon-lined stainless steel container and kept at 120 °C for 1 days. After cooling to room temperature, the MAF-X8 coated fiber was washed gently with methanol, and heated at 250 °C in the GC injection port for 20 min to remove guests from the films. The thickness of the MAF-X8 films was measured by SEM.

SPME procedures

All SPME fibers were pretreated in the GC injection port at 250 °C under nitrogen flow for 15 min before use. All the appropriate standard solutions were prepared by diluting the BTEX or Phenols stock solution (1 mg/mL) with saturated sodium chloride solution. A glass vial (40 mL), the sample container, with a magnetic bar inside was placed on a stirring platform with a stirring rate of 1500 rpm. Then the needle of the SPME fiber was penetrated the septum of the vial and the coated fiber was exposed to the standard sample vapor for a

period of time at room temperature. After extraction, the fiber was subsequently inserted into the GC injector for desorption and analysis.

GC-MS analysis

GC-MS analysis was performed on a Hewlett–Packard 6890N gas chromatograph (Agilent Technologies, CA, USA) equipped with a MSD 5975 mass spectrometer (Agilent Technologies) and a split/splitless injector. Chromatographic separation was carried out with a HP-5MS 5% phenyl-/95% methylsiloxane capillary (30 m×250 μ m, 0.25 μ m). In all measurements, the constant flow rate of helium carrier gas was kept at 1.2 mL/min and the injector temperature was 250 °C with splitless. The initial oven temperature was 70 °C, and then increased to 140 °C at a rate of 10 °C/min. The total run time was 12 min.

X-ray single-crystal structure analyses.

Diffraction data were collected using a Bruker Apex CCD area-detector diffractometer (Mo-K α). Absorption corrections were applied by using the multi-scan program SADABS.^{S2} The structures were solved by direct methods and refined with the full-matrix least-squares method on F^2 by the SHELXTL crystallographic software package.^{S3} The structures are all pseudo merohedral twin crystals. Hydrogen atoms were placed geometrically. All non-hydrogen atoms of the host frameworks were refined anisotropically. The guest mesitylene molecules were slightly disordered, and their occupancies were obtained from refinement. Crystal data and details of data collection and refinements of the compounds were listed in table S1. CCDC 892987 and 892988 contain the supplementary crystallographic data for this paper. These data can be obtained free of charge from The Cambridge Crystallographic Data Centre via www.ccdc.cam.ac.uk/data_request/cif.

Computational details

All calculations were performed in the MS modeling 5.0 package.^{S4} The saturation/maximum uptakes of mesitylene, toluene and 2-chlorophenol were simulated at 298 K using the GCMC (Grand Canonical Monte Carlo) method. The fixed pressure task and Metropolis method in Sorption program and the universal forcefield (UFF) were adopted. The simulation box representing MAF-X8 contains 8 ($2 \times 2 \times 2$) unit cells while the framework and all the guest molecules were considered to be rigid. Partial charges were produced the same as MM modeling mentioned above. The cutoff radius was chosen as 12.8 Å for the LJ interactions, and the long-range electrostatic interactions were handled using the Ewald & Group summation method. For each state point, 5.0×10^6 equilibration steps were used, followed by 5.0×10^6 production steps for computing the ensemble averages.

To further explain the different adsorption kinetics, we calculated the diffusion barriers of guest molecules passing through the 1D channels. Corresponding with the TGA (Fig. S10), 2-chlorophenol and toluene were used as probe molecules in the modeling. Firstly, we used the Sorption module, Locate task and Metropolis method to identify the relatively favored sorption location of the probe molecules, then taken it as a starting point and let the probe molecules pass through the framework channel along the channel direction step by step. For every step, geometry optimization was taken by the Forcite module to obtain the total energy and then calculated the interaction energy between probe molecule and framework by the following equation:

$$E_{\text{interaction}} = E_{\text{total}} - E_{\text{framework}} - E_{\text{probe}} \quad (\text{eq-1})$$

Where E_{total} is the total energy of the framework and probe molecule, while $E_{\text{framework}}$ and E_{probe} denote the energies of the framework and probe molecule respectively. So, we can draw an energy curve and the difference between the maximum and minimum energy referred to as the diffusion barrier (Fig. 8). Partial charges for atoms of the framework and the probe molecules were derived from QEq method and QEq neutral 1.0 parameter. All parameters for atoms of MAF-X8 and probe molecules were modeled with the universal force field (UFF) embedded in the MS modeling 5.0. The optimization step was performed

with a cutoff radius of 18.5 Å, and a smart algorithm was applied. For the sake of making a comparison, we performed a similar modeling for the reported structure Zn(BDP) (BDP = 1,4-benzenedipyrazolates).

In order to simulate the host-guest interaction on the crystal surface, we cleaved a (100) surface of MAF-X8 with a 10 Å vacuum slab placed upon it and a probe molecule was placed on the surface. This structural model was then energy-minimized maintaining fixed the atomic coordinates of the surface. As the molecular mechanics (MM) is hard to accurately simulate the hydrogen bond, the interactions between probe molecules and the crystal surface were calculated by density functional theory (DFT) through the Dmol³ module. The widely used generalized gradient approximation (GGA) with the Perdew–Burke–Ernzerhof (PBE) functional and the double numerical plus polarization (DNP) basis set as well as the effective core potential (ECP) were used. The binding energy was calculated similar to equation eq-1.

Table S1 Crystallographic data and structure refinement details for MAF-X8.

Complex	[Zn(mpba)]·0.76C ₉ H ₁₂	[Zn(mpba)]
formula	C _{18.87} H _{19.16} N ₂ O ₂ Zn	C ₁₂ H ₁₀ N ₂ O ₂ Zn
Formula weight	371.31	279.61
Temperature /K	123(2)	293(2)
Crystal system	orthorhombic	orthorhombic
Space group	<i>Ibca</i> (No.73)	<i>Ibca</i> (No.73)
<i>a</i> (Å)	13.9562(9)	13.9249(12)
<i>b</i> (Å)	23.5904(15)	23.653(2)
<i>c</i> (Å)	23.5858(15)	23.637(2)
<i>V</i> (Å ³)	7765.2(9)	7785.3(11)
<i>Z</i>	16	16
<i>D_c</i> /g cm ⁻³	1.271	0.954
μ/mm ⁻¹	1.281	1.255
<i>R</i> ₁ [<i>I</i> > 2σ(<i>I</i>)] ^[a]	0.0734	0.0538
<i>wR</i> ₂ [<i>I</i> > 2σ(<i>I</i>)] ^[b]	0.1920	0.1381
<i>R</i> ₁ (all data)	0.0880	0.0675
<i>wR</i> ₂ (all data)	0.2058	0.1505
GOF	1.025	1.030

$$^{[a]} R_1 = \frac{\sum ||F_o| - |F_c||}{\sum |F_o|}, \quad ^{[b]} wR_2 = \left[\frac{\sum w(F_o^2 - F_c^2)^2}{\sum w(F_o^2)^2} \right]^{1/2}.$$

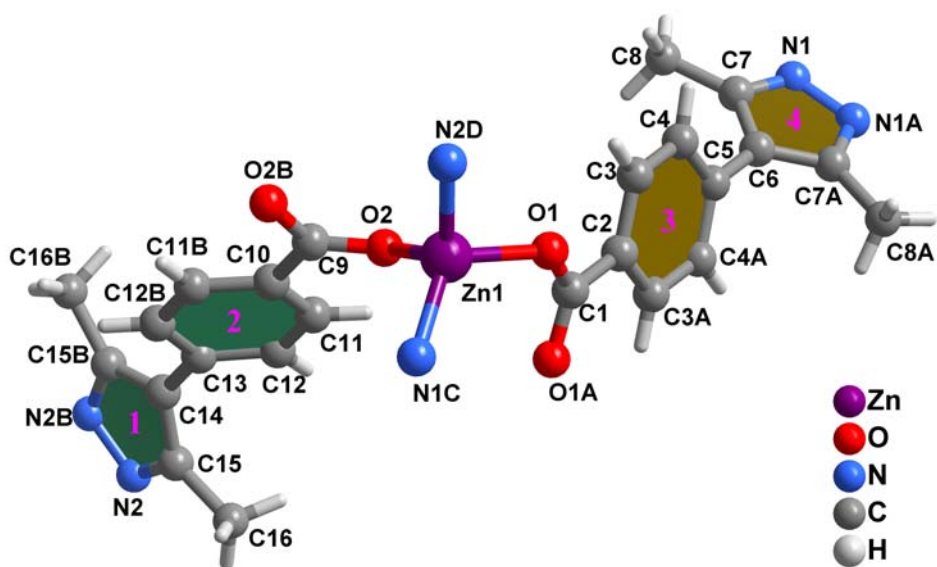


Fig. S1 Perspective view of coordination environments of MAF-X8. Symmetric codes: A = $1-x, 0.5-y, z$; B = $0.5-x, y, 1-z$; C = $x, 0.5-y, -0.5+z$; D = $x, -0.5+y, 1-z$. Dihedral angle between plane 1 and plane 2 is 52.5° ; between plane 3 and plane 4 is 61.2° .

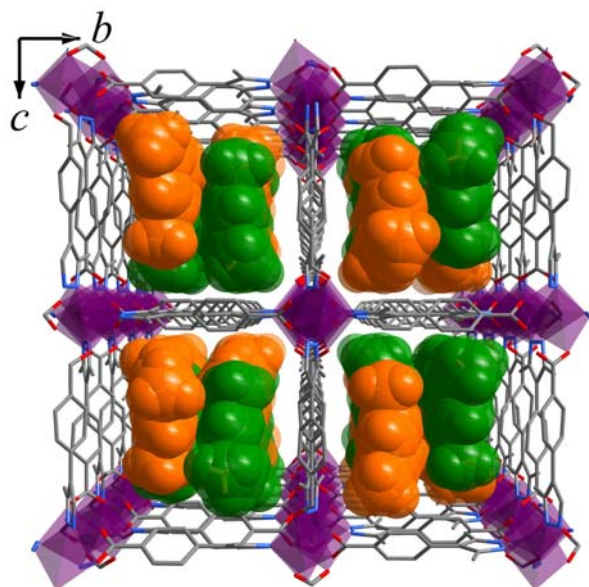


Fig. S2 Perspective view of the structure of mesitylene loaded MAF-X8 (the mesitylene molecules are highlighted in space-filling mode).

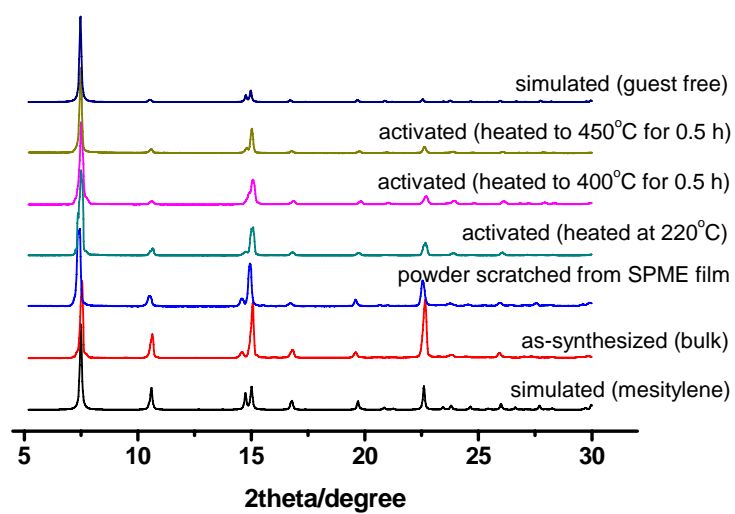


Fig. S3 PXR D patterns for MAF-X8.

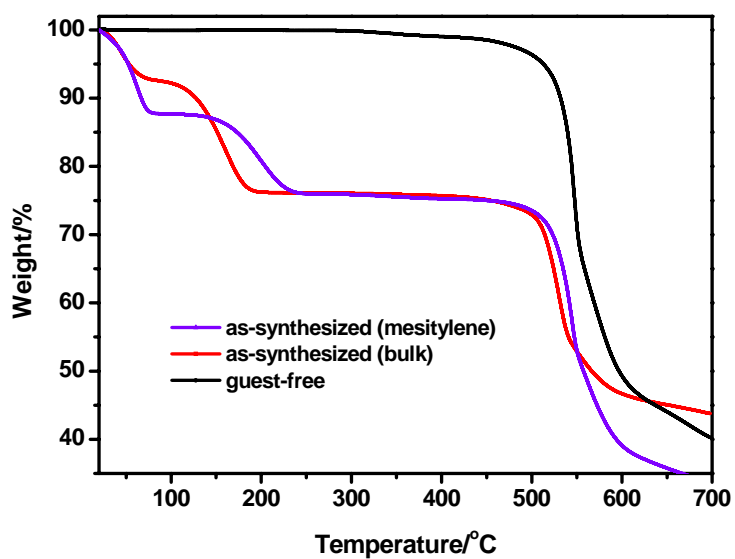


Fig. S4 TGA curve for MAF-X8. The weight loss of 24.6% corresponds to formula $[\text{Zn}(\text{mpba})] \cdot 0.76\text{C}_9\text{H}_{12}$.

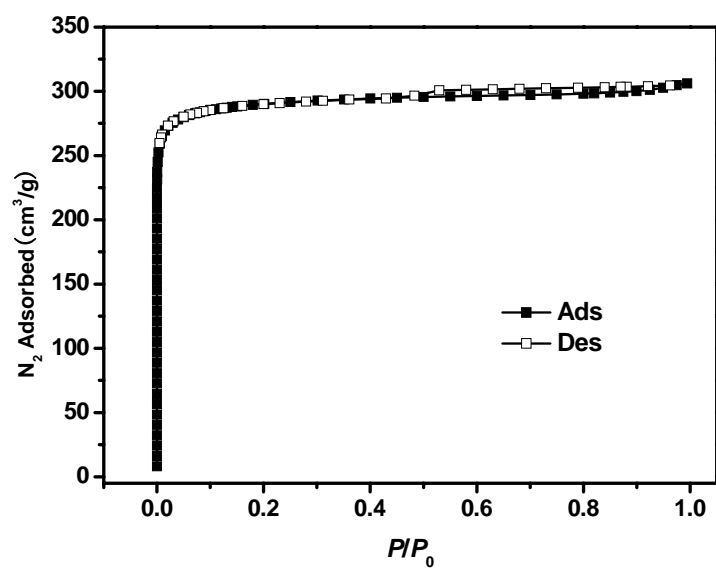


Fig. S5 N₂ sorption isotherm of MAF-X8 at 77 K.

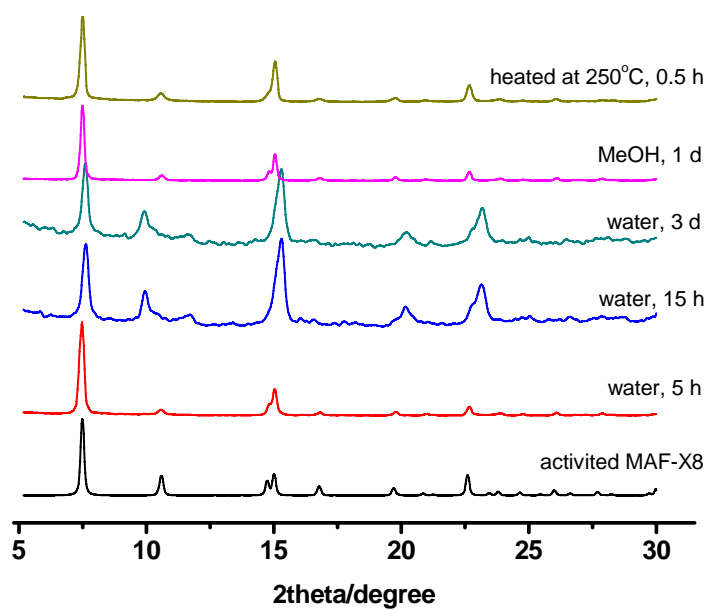


Fig. S6 PXRD patterns for activated MAF-X8 exposed to saturated water vapor for different time and subsequent restoration of the water-treated samples by MeOH vapor or by direct heating.

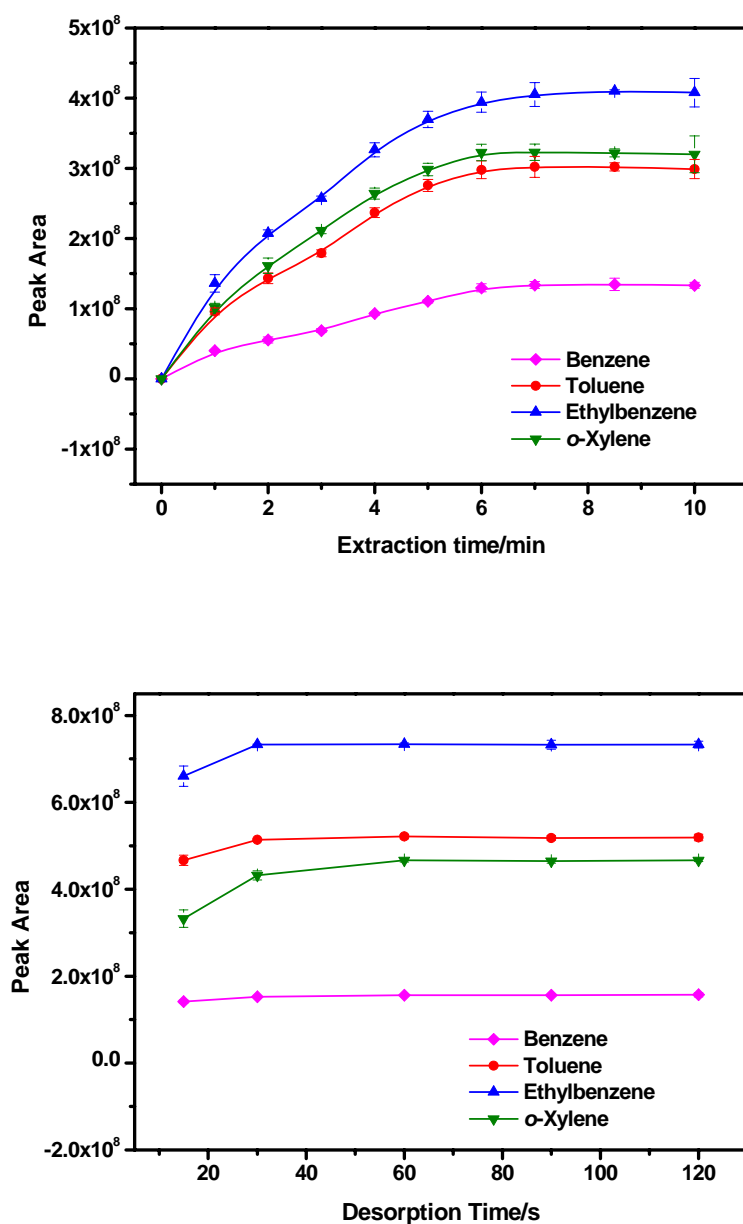


Fig. S7 (top) adsorption and (bottom) desorption kinetics of the MAF-X8 coated SPME fiber tested by 200 ng/mL BTEX. The error bar shows the standard deviation of triplicate extractions.

Table S2 The limits of detection (LODs), linear range and the relative standard deviation (RSD).

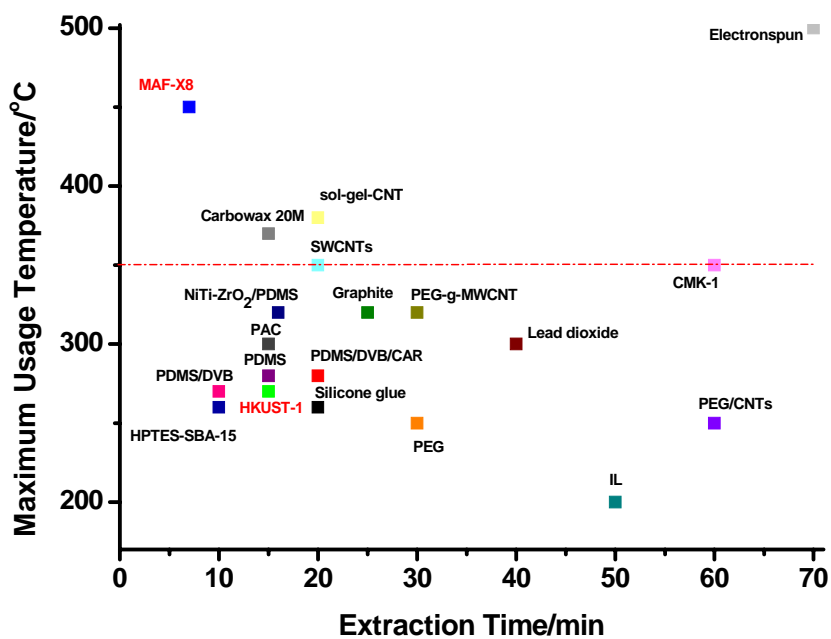
analyte	LOD ($\mu\text{g/L}$, S/N=3)	linear range ($\mu\text{g/L}$)	linearity (R^2)	repeatability (%, n = 6)	fiber-to-fiber reproducibility (%, n =3)
Benzene	0.060	0.40-500	0.9976	2.6	8.0
Toluene	0.013	0.10-300	0.9988	1.3	4.9
Ethylbenzene	0.006	0.10-300	0.9989	0.9	7.3
<i>o</i> -Xylene	0.007	0.10-300	0.9999	4.1	6.7

Table S3 Comparison of the major parameters for various SPME fibers in determination of BTEX compounds.

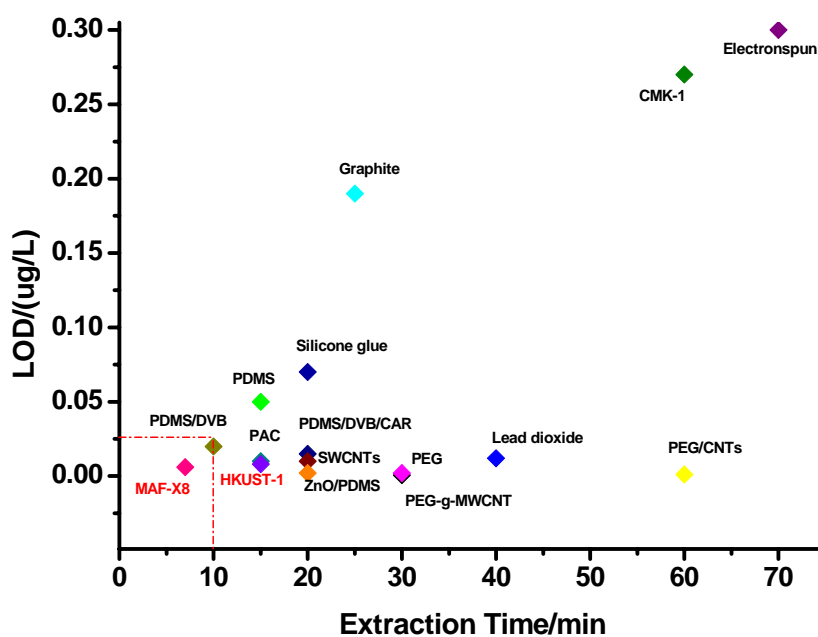
Fiber coating	Extraction time (min)	Maximum usage temperature (°C)	LOD (µg/L)	Linear range (µg/L)	Reference
PEG-g-MWCNTs	30	320	0.0006-0.003	0.206-1.04	S5
NiTi-ZrO ₂ -PDMS	16	320	0.6-1.6	2-200	S6
PDMS	15	280	0.05-0.28	2-200	S7
Lead dioxide	40	300	0.012-0.054	0.1-100	S8
Graphite	25	320	0.19-3.29	0.6-11240	S9
Disposable ionic liquid (IL)	50	200	100-800	400-60000	S10
HPTES-SBA-15	10	260	1-13	100-500000	S11
PEG	30	250	0.002-0.8	0.005-2000	S12
PEG/nano tube	60	250	0.001-0.8	0.002-2000	S12
PDMS/DVB	10	270	0.02-0.07	NR	S13
PDMS/DVB/CAR	20	280	0.015-0.26	0.049-3.7	S14
Electrospun	70	>500	0.3-1.0	0.05-40	S15
Carbowax 20M	15	370	NR	NR	S16
Sol-gel-CNT	20	380	NR	100-2500	S17
SWCNTs	20	350	0.01-0.026	0.5-50	S18
CMK-1	60	350	0.27-1.1	1-800	S19
PAC	15	300	0.01-0.94	50-14000	S20
Silicone glue	20	260	0.07-0.17	0.5-10000	S21
ZnO/PDMS	20	NR	0.002-0.005	0.02-200	S22
HKUST-1	15	270	0.0083-0.0233	0.072-18	S23
MAF-3	NR	380	NR	NR	S24

MAF-4	NR	480	NR	NR	S24
MAF-X8	7	450	0.006-0.060	0.01-500	This work

NR = Not reported.



(a)



(b)

Fig. S8 Comparison of the major parameters for various SPME fibers in determination of BTEX compounds. (a) Extraction time vs maximum usage temperature (The red line presents the general maximum usage temperature of the GC injection port). (b) Extraction time vs the lowest LOD.

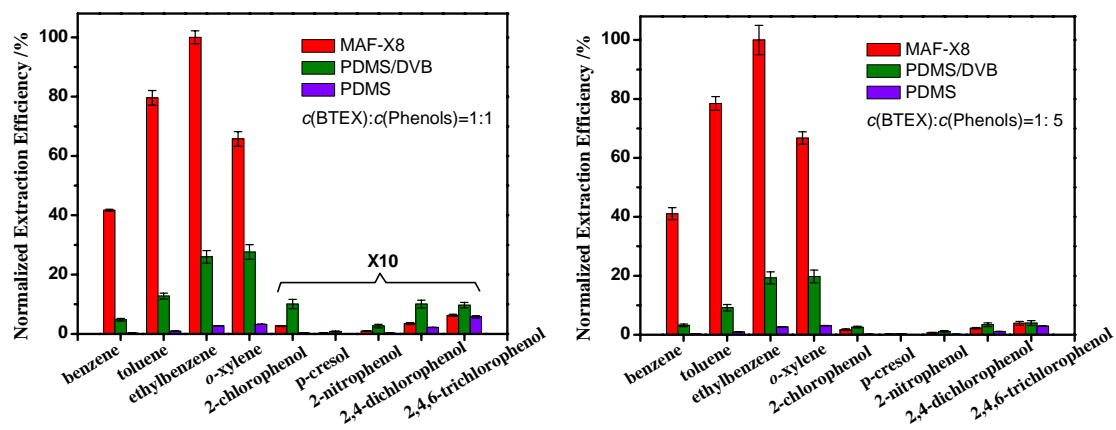


Fig. S9 Comparison of the normalized extraction efficiencies of MAF-X8 coated fiber and commercial SPME fibers for BTEX/Phenols mixtures at 1:1 (left, extraction efficiencies are multiplied by 10 for the Phenols) and 1:5 (right). The error bar shows the standard deviation of the mean.

Table S4 Plotted data for Fig. 4 and Fig. 5.

Peak area/coating volume	benzene	toluene	ethylbenzen e	o-xylene	2-chlorop henol	p-cresol	2-nitrophe nol	2,4-dichlo rophenol	2,4,6-trich lorophenol	
MAF-X8	1:0	166804317	287781709	365183859	238142044	0	0	0	0	
	Normalized/%	45.57354	78.62645	99.77392	65.06411	0	0	0	0	
	1:1	152616942	291174950	366011334	240599070	968288	97399	353003	1273283	2289263
	Normalized/%	41.69733	79.55353	100	65.73542	0.26455	0.02661	0.09644	0.34788	0.62546
	1:5	146465260	279977055	356747462	238147319	6139603	706510	2455555	7960127	13742220
	Normalized/%	40.01659	76.49409	97.46897	65.06556	1.67743	0.19303	0.67089	2.17483	3.75458
PDMS/DYB	1:0	55077279	144867555	290709411	309838531	0	0	0	0	
	Normalized/%	17.77612	46.75582	93.82610	100	0	0	0	0	
	1:1	46857531	126177554	256842714	273030497	9943747	823760	2607537	9956679	9576806
	Normalized/%	15.12321	40.72365	82.89567	88.12025	3.20933	0.26586	0.84157	3.21350	3.09090
	1:5	30987656	88203111	175758100	179659641	24796193	2648416	12329759	35497521	41403322
	Normalized/%	10.00123	28.46744	56.72571	57.98493	8.00294	0.85477	3.97941	11.45678	13.36287
PDMS	1:0	5299859	18948547	55650825	65091507	0	0	0	0	
	Normalized/%	8.14217	29.11063	85.49629	100	0	0	0	0	
	1:1	4776009	16889505	50087062	58868532	598514	142757	439824	3953736	10546899
	Normalized/%	7.33738	25.94732	76.94869	90.43965	0.91950	0.21932	0.67570	6.07412	16.20319
	1:5	4666064	15916491	47219651	55490947	3085325	775025	2893985	19540390	51486588
	Normalized/%	7.16847	24.45248	72.54349	85.25067	4.73998	1.19067	4.44603	30.01988	79.09878

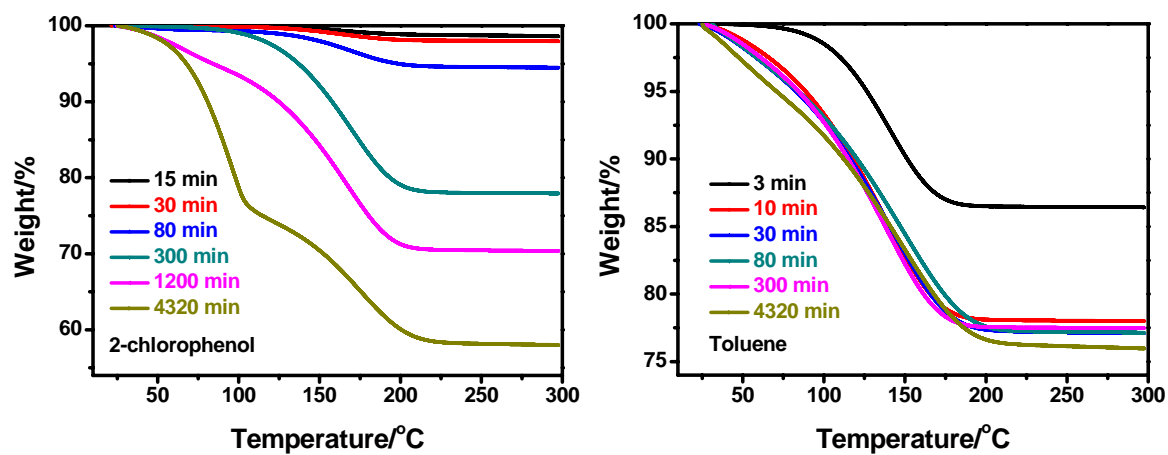


Fig. S10 TGA curves for MAF-X8 after exposed to 2-chlorophenol or toluene vapor for different time.

Table S5 Comparison of the theoretical/observed saturation/maximum uptakes of mesitylene, toluene and 2-chlorophenol for MAF-X8.

Adsorbate	mesitylene	toluene	2-chlorophenol
Liquid density ρ_G (g/cm ³)	0.864	0.866	1.24
Empirical uptake ^a	45.3%	45.4%	65.0%
(Corresponding TGA weight loss ^b)	(31.2%)	(31.2%)	(39.4%)
[Corresponding guest molecule per Zn]	[1.05]	[1.38]	[1.41]
(Observed TGA weight loss)	(24.6%)	(24.0%)	(42.0%)
Corresponding uptake ^c	32.6%	31.6%	72.4%
[Corresponding guest molecule per Zn]	[0.76]	[0.96]	[1.57]
Molecular modeling uptake	32.3%	33.0%	46.0%
(Corresponding TGA weight loss ^b)	(24.4%)	(24.8%)	(31.5%)
[Corresponding guest molecule per Zn]	[0.75]	[1]	[1]

^a uptake = $0.524 \text{ cm}^3/\text{g} \times \rho_G$

^b weight loss = uptake/(1 + uptake)

^c uptake = weight loss / (1 – weight loss)

REFERENCES

- S1 C. Foces-Foces, C. Cativiela, M. M. Zurbano, I. Sobrados, N. Jagerovic, J. Elguero, *J. Chem. Crystallogr.*, 1996, **26**, 579-584.
- S2 G. M. Sheldrick, *SADABS 2.05*, University Göttingen, Göttingen, Germany, 2002.
- S3 *SHELXTL 6.12*, Bruker Analytical Instrumentation, Madison, WI, 2000.
- S4 *Accelrys, Materials Studio Getting Started, release 5.0*, Accelrys Software, Inc., San Diego, CA, 2009.
- S5 A. Sarafraz-Yazdi, A. Amiri, G. Rounaghi, H. E. Hosseini, *J. Chromatogr. A*, 2011, **1218**, 5757-5764.
- S6 D. Budziak, E. Martendal, E. Carasek, *J. Chromatogr. A*, 2008, **1187**, 34-39.
- S7 A. Gaujac, E. S. Emídio, S. Navickiene, S. L. C. Ferreira, H. S. Dórea, *J. Chromatogr. A*, 2008, **1203**, 99-104.
- S8 A. Mehdinia, M. F. Mousavi, M. Shamsipur, *J. Chromatogr. A*, 2006, **1134**, 24-31.
- S9 F. Luo, Z. Wu, P. Tao, Y. Cong, *Anal. Chim. Acta*, 2009, **631**, 62-68.
- S10 J.-f. Liu, N. Li, G.-b. Jiang, J.-m. Liu, J. Å. Jönsson, M.-j. Wen, *J. Chromatogr. A*, 2005, **1066**, 27-32.
- S11 P. Hashemi, M. Shamizadeh, A. Badiei, P. Z. Poor, A. R. Ghiasvand, A. Yarahmadi, *Anal. Chim. Acta*, 2009, **646**, 1-5.
- S12 A. Sarafraz-Yazdi, H. Piri moghadam, Z. Es'haghi, S. Sepehr, *Anal. Methods*, 2010, **2**, 746.
- S13 I. Arambarri, M. Lasa, R. Garcia, E. Millán, *J. Chromatogr. A*, 2004, **1033**, 193-203.
- S14 C. M. M. Almeida, L. V. Boas, *J. Environ. Monit.*, 2004, **6**, 80-88.
- S15 J. W. Zewe, J. K. Steach, S. V. Olesik, *Anal. Chem.*, 2010, **82**, 5341-5348.
- S16 R. G. da Costa Silva, F. Augusto, *J. Chromatogr. A*, 2005, **1072**, 7-12.
- S17 R. Jiang, F. Zhu, T. Luan, Y. Tong, H. Liu, G. Ouyang, J. Pawliszyn, *J. Chromatogr. A*, 2009, **1216**, 4641-4647.
- S18 Q. Li, X. Ma, D. Yuan, J. Chen, *J. Chromatogr. A*, 2010, **1217**, 2191-2196.
- S19 M. Anbia, M. Khazaei, *Chromatographia*, 2011, **73**, 379-384.
- S20 W. Shutao, W. Yan, Y. Hong, Y. Jie, *Chromatographia*, 2006, **63**, 365-371.
- S21 D. Panavaitė, A. Padarauskas, V. Vičkačkaitė, *Anal. Chim. Acta*, 2006, **571**, 45-50.
- S22 D. Wang, Q. Wang, Z. Zhang, G. Chen, *The Analyst*, 2012, **137**, 476.
- S23 X.-Y. Cui, Z.-Y. Gu, D.-Q. Jiang, Y. Li, H.-F. Wang, X.-P. Yan, *Anal. Chem.*, 2009, **81**, 9771-9777.
- S24 N. Chang, Z.-Y. Gu, H.-F. Wang, X.-P. Yan, *Anal. Chem.*, 2011, **83**, 7094-7101.